Review of Wearable Antennas for WBAN Applications

J. C. Wang, E. G. Lim, M. Leach, Z. Wang and K. L. Man

Abstract—**Recent research into wearable antennas has provoked increasingly widespread concern about the use of wireless body area network (WBAN) applications. This paper reviews state-of-the-art wearable antennas on textile materials focusing on designs with dual band and UWB and wearable antennas with metamaterials with single band and dual band. This paper also presents the challenges and considerations when designing a suitable wearable antenna.**

Index Terms—**Wearable antennas， patch antennas， textile antennas， metamaterials, WBAN applications**

I. Introduction

WIRELESS body area network (WBAN) technology has the potential to provide an unprecedented opportunity for ubiquitous real-time healthcare and fitness monitoring in ambulances, emergency rooms, operating theatres, postoperative recovery rooms, clinics, homes and even on the move; such that many diseases could be prevented through early detection and doctors could give patients efficient advice on improving their health [1]. In recent years, there has been increasing concern about the safety of WBAN systems, particularly wearable electronics, over a multitude of applications including medical, entertainment and military. A key feature of these wearable electronics is that they have to allow wireless communications from or to the body via conformal and wearable antennas. Therefore, wearable antennas play a pivotal role in wireless on-body centric communications and arouse significant attention in research. Since wearable antennas operate in close proximity to the human body, the loading effect due to the lossy nature of body tissues coupled with their high dielectric constants and conductivity makes the design of a high radiation efficiency antenna challenging. This is compounded by the desire and requirement for such antennas to be light weight, low cost, be maintenance-free and require no installation.

Manuscript received July 19th, 2016; revised August 9th, 2016. This work is partially supported by the Natural Science Foundation of Jiangsu province (No. BK20131183) and XJTLU Research Development Fund (RDF-14-03-24 and RDF-14-02-48).

J. C. Wang is with the Jiaotong-Liverpool University, China. Email: Jingchen.Wang@xjtlu.edu.cn

E. G. Lim is with the Xi'an Jiaotong-Liverpool University, China. Email: enggee.lim@xjtlu.edu.cn

M. Leach is with the Jiaotong-Liverpool University, China. Email: mark.leach@xjtlu.edu.cn

Z. Wang is with the Xi'an Jiaotong-Liverpool University, China. Email: zhao.wang@xjtlu.edu.cn

K. L. Man is with the Xi'an Jiaotong-Liverpool University, China. Email: ka.man@xjtlu.edu.cn

One of the dominant research focuses in wearable antennas for WBAN applications is the patch antenna, due to its relatively high directivity, as a result of the large ground plane used in its design. Besides the directivity, microstrip patch antennas have some significant advantages for on-body wearables, the three major ones being: their ease of construction, their cost effectiveness and the relative isolation achieved between the radiating element and the body due to the ground plane, which leads to a significant reduction in energy absorbed by the body. [2]. However, patch antennas tend to be low bandwidth and may need to be relatively large if they are to be robust against perturbation by the body [3].

With the development of wearable antennas, studies on patch antennas have mainly focused on flexible materials. The properties of the materials used can influence the behavior of the antenna employed. For example, the bandwidth and the efficiency of a planar microstrip antenna are mainly determined by the permittivity and the thickness of the substrate [4]. The use of textiles in wearable antennas requires the characterization of their properties. Electro-textiles are conductive fabrics constructed by mixing conductive metal or polymer threads with normal textiles. These fabrics, which are wearable, durable and flexible, make it suitable for wearable contexts. The conductive textile is expected to have low and stable electrical resistance to minimize losses. The flexibility of the materials is also needed so that the antenna can be deformed over the cloth. Substrate selection is a critical step in designing a textile or wearable antenna, in order to be robust for a specific application. In general, textiles present a considerably low dielectric constant that reduces the surface wave losses and increases the impedance bandwidth of the antenna [5].

On the other hand, metamaterials such as artificial magnetic conductor (AMC) surfaces, high impedance surfaces (HIS) or the electromagnetic bandgap (EBG) structures have emerged as promising designs for wearable antennas. Metamaterials are artificial materials engineered to have properties that may not be found in nature. They are assemblies of multiple individual elements fashioned from conventional microscopic materials such as metals or plastics, but the materials are usually arranged in repeating patterns [6]. Metamaterials are of many attractive features in general. They can improve the overall matching and thus radiation from small antennas [7] and reduce the specific absorption rate (SAR) in the head [8]. They can also control the electromagnetic near fields around the antenna. This can be exploited to reduce the absorbed power in the human body tissues.

This paper is an extended version of [9]. A review of wearable textile antennas with patch structures and metamaterials will be presented in Section II. Section III and IV provide some challenges or considerations for wearable

(Advance online publication: 26 November 2016)

antennas and the conclusion of this paper, respectively.

II. WEARABLE PATCH ANTENNAS

A. *Conformal Wearable Antenna*

On-body Textile Antenna

A microstrip on-body antenna with probe-feed excitation is presented in [10]. The design of a proposed planar on-body antenna along with its dimensions is shown in Fig. 1(a), and the manufactured prototype is shown in Fig. 1(b). The antenna has been designed and fabricated using jean as the substrate and copper tape as the patch radiating element and ground, to provide flexibility to the conformal antenna. The jean material used has a relative permittivity of l.68, a loss tangent of 0.01 and a thickness of 1 mm. Slots in an antenna have been designed to attain adequate bandwidth, high gain and to have minimum antenna parameter variation when in close proximity to the human body.

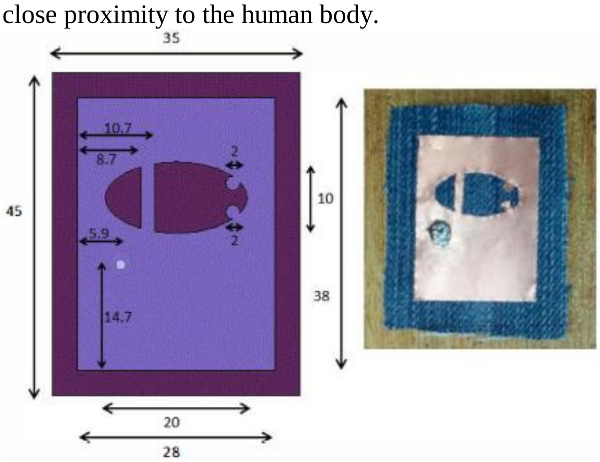

(a) Simulated Design (b) Fabricated Prototype

Fig.1. Proposed Antenna with dimensions in millimeters

For near body effects analysis in HFSS, an antenna of average clothing thickness has been placed at a 5 mm distance from a body phantom. Air has been used between the textile antenna and body model (skin, fat, muscle and bone), but this air spacing size has very little effect on antenna performance. The near body performance analysis setup is shown in Fig. 2.

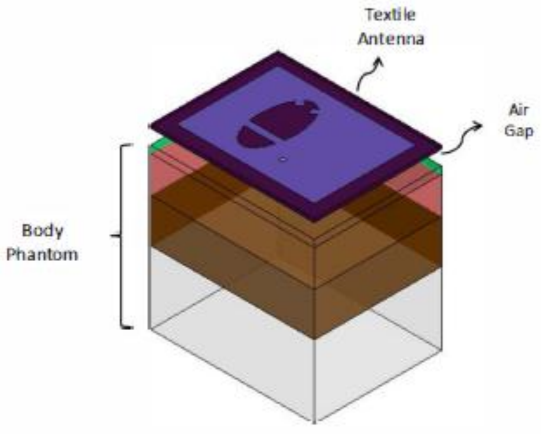

Fig. 2. Near body performance analysis setup

Simulated and Measured return loss results for the proposed antenna both with and without the presence of a body phantom are presented in Fig. 3.

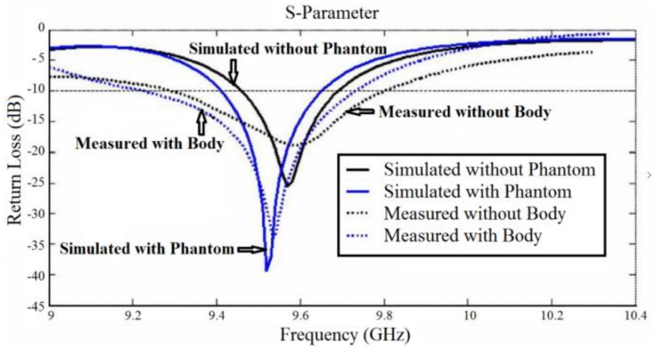

Fig. 3. Simulated and Measured S-11 of proposed antenna with and without near body effects

The results show that the antenna is suitable for function and is efficient over a 200 MHz band from 9.45 to 9.65 GHz. Over this band, the proposed antenna achieved reasonably high gains of 12.8 dB and 13.2 dB with and without body phantom respectively [10].

Dual Band Diamond Textile Wearable Antenna

The diamond-shaped dipole antenna is another option for wearable applications, able to offer improved bandwidth and efficiency over the standard dipole. The combination of two diamond-shaped dipole antennas offers the possibility for dual band use and increased bandwidth. Fig. 4 shows the commercially available electro textile diamond-shaped dipole dual antenna, it has a dielectric constant of 1.7, copper foil tape, which has high conductivity of 5.88×10^7 and a thickness of 0.035 mm as the conducting element [11].

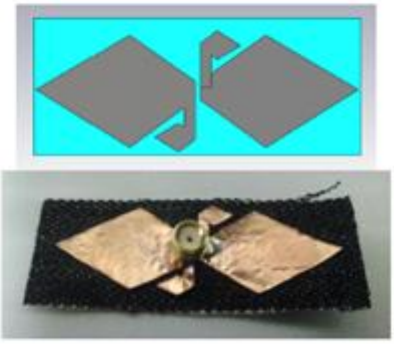

Fig. 4. Dual wideband textile antenna design using CST and prototype of denim antenna

Using the CST software with its built in Gustav male model, a simulation is developed to investigate the performance of the textile antenna. The antenna performance is investigated under three conditions: free space (no body phantom), 3 mm from the backside of the phantom (shown in Fig. 5) and in the same position but with the 3 mm gap filled by a layer of wash cotton (clothes) (permittivity 1.51 and loss tangent of 0.021 at 2.45 GHz) [12].

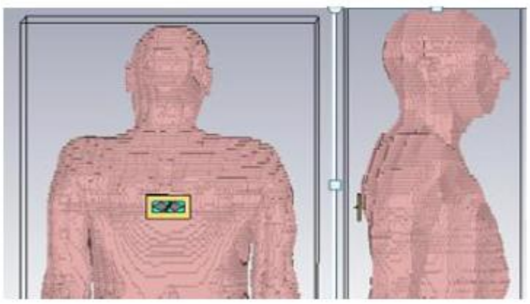

Fig. 5. Location of antenna at the backside of Gustav body

Fig. 6 shows that, the presence of the phantom and clothing (wash cotton) exhibits little frequency detuning or fluctuation in bandwidth around the dual designed resonances at 2.45 GHz and 5.8 GHz. Placing the antenna on the backside of the body results in an immediate 85% drop (from 99% to 14%) in efficiency at 2.45 GHz and 23.5% (from 96% to 72.5%) at 5.8GHz [11].

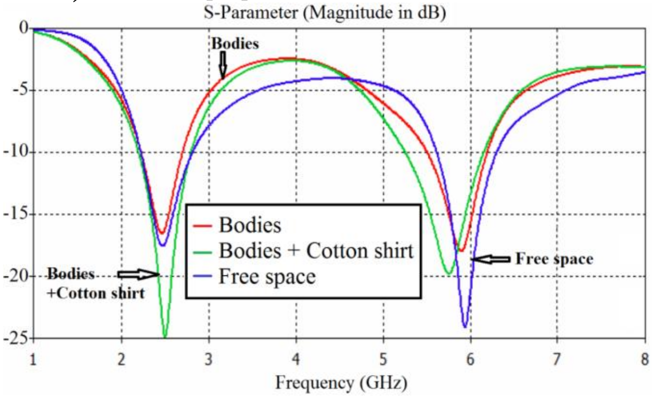

Fig.6. Simulated return loss result of the textile antenna blue (with bodies and cotton clothes), red (free space) and green (with bodies)

Polygon-Shaped Slotted Dual-band Antenna

To reduce the patch area and increase the electrical length, a polygon-shaped patch antenna with a ring-shaped slot was proposed in [13] to operate within the two mobile frequency bands, GSM-900 and GSM-1800. The designed patch antenna consists of a substrate located in between ground plane and patch. The material used for ground plane and patch is copper. The substrate is jean fabric that has a thickness of 1 mm, dielectric constant 1.7, and loss tangent 0.025 [14]. The photograph of the handmade prototype is given in Fig. 7.

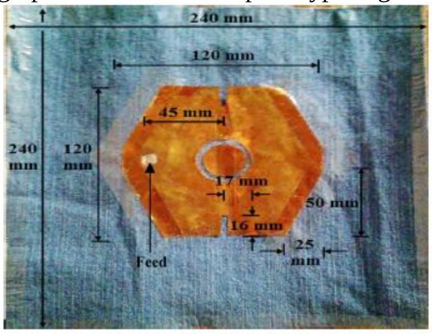

Fig. 7. Fabricated prototype of the proposed dual-band antenna

The simulated and measured plots for free space and on-body measurements are shown in Fig. 8. The directivity values at the higher and lower resonant frequencies are 8.1 and 7.4 dBi, respectively. The corresponding radiation (total) efficiencies are 20.5% (16.7%) and 10.3% (4.7%) [13].

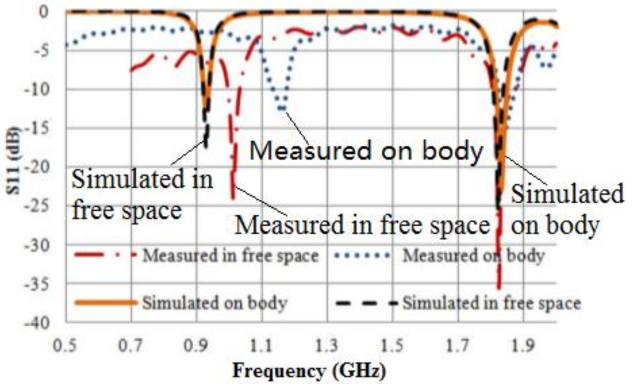

Fig. 8. Simulated and measured (free space and on-body) S11 response

Small Planar UWB Wearable Antenna

A small planar UWB wearable antenna proposed in [15], consists of a substrate made of jean and a metallic radiator (adhesive copper tape). The average values of the dielectric constant and loss tangent are 1.76 and 0.078 respectively. Fig. 9 shows the fabricated antenna.

(a) (b)

Fig. 9. Prototype of the proposed antenna, a) front and b) back views

A portion of the human arm was selected as the antenna location and the appropriate phantom section chosen for simulation in CST. Fig. 10 illustrates the top and front view of the phantom with four layers (skin, fat, muscle and bone). The resulting S_{11} parameters are shown in Fig. 11 with acceptable bandwidth achieved from 3 to 4.5 GHz and from 6.5 to 11.5 GHz. The antenna achieves a good efficiency reaching higher than 65% at the higher end of the UWB band [15].

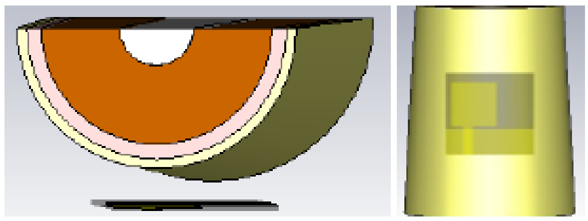

Fig. 10. Human arm model developed in CST MWS, a) top view, b) front view

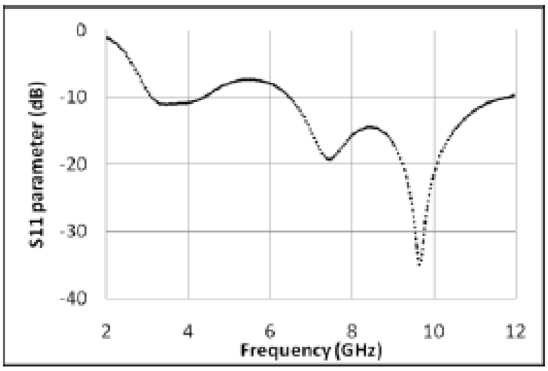

Fig.11. S11 parameter at 5 mm far from the arm model

Compact UWB Wearable Antenna

By combining slot and truncation techniques, the impedance bandwidth of the proposed patch antenna has been improved in [16]. A flexible textile substrate (jean) with metallic radiator (adhesive copper tape) is used for construction of the wearable antenna with a dielectric constant of 1.76 and loss tangent of 0.078. The fabricated antenna is shown in Fig. 12.

(a) (b)

Fig. 12. Prototype of the proposed antenna (a) front view (b) back view

Fig. 13 shows the simulated return loss for the antenna in the presence of the human body. The human body phantom here is a conical-shaped arm model consisting of skin, fat, muscle and bone. Taking the upper frequency limit as 10.6 GHz and lower frequency as 4.2 GHz, the improved bandwidth covers up to 86.48% [16]. The gains at the maximums are 2.74 dB at 3.0 GHz, 4.17 dB and 4.07 dB at 7.0 GHz and 9.0 GHz respectively.

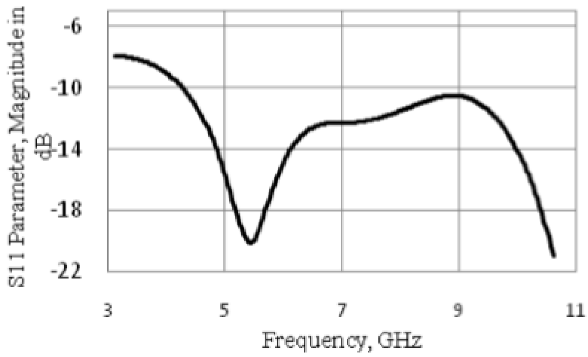

Fig. 13. S11 parameter at the presence of human body

B. *Metamaterial antenna*

Wearable AMC Backed Near-endfire antenna

An endfire planar Yagi-Uda antenna backed with AMC structure has been presented on a flexible latex substrate in [17]. A conventional planar Yagi antenna is used for endfire radiation at 2.4 GHz. The optimized dimensions for the driver, director and reflector elements are shown in Fig. 14.

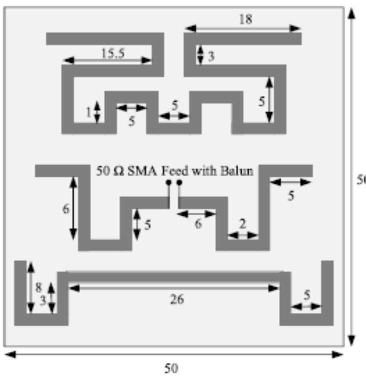

Fig. 14. Proposed endfire Yagi-Uda antenna (with optimized dimension for the director, driver and reflector elements unit: millimeter)

The bidirectional-endfire radiation of the Yagi antenna is altered to provide off-axis near endfire radiation using the 0° reflection phase single AMC surface (S-AMC) with 3×3 unit AMC array. The final optimized dimensions are also shown in Fig. 15(a). The in-house fabricated FR-4 prototype of the S-AMC metasurface for verifying the concept is shown in Fig. 15(b).

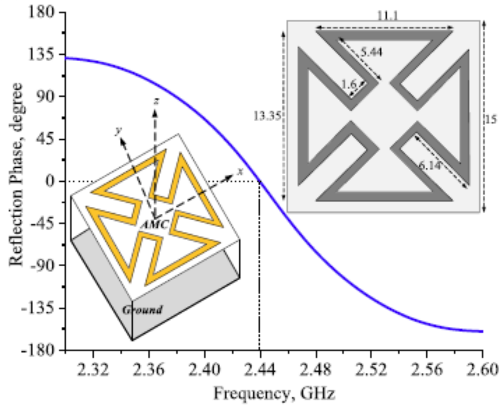

(a)

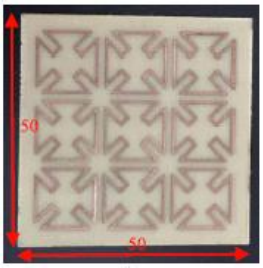

(b)

Fig. 15. (a) Reflection phase graph of AMC unit cell with the AMC unit-cell structure (b) Fabricated FR4 PCB prototype to realize the S-AMC metasurface design for verifying the concept (unit: millimeter).

Another configuration of this near-endfire Yagi-Uda antenna is backed by double-layered AMC (D-AMC) which includes the lower AMC surface layer with an array of 4×4 units and the upper AMC layer with an array of 3×3 units. The final optimized AMC unit dimensions for a D-AMC surface having 0° reflection phase at 2.4 GHz are shown in Fig. 16(a). The in-house fabricated FR-4 prototypes of the D-AMC metasurface for verifying the concept are shown in Fig. 16(b).

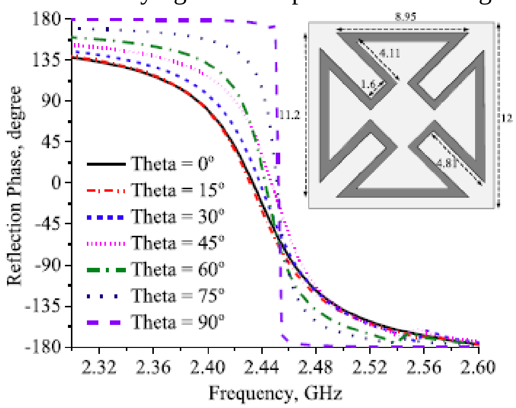

(a)

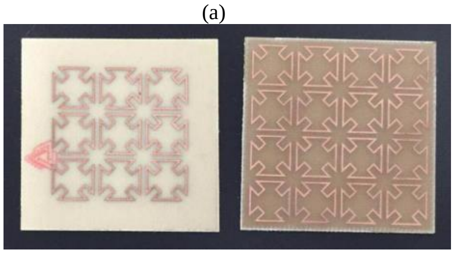

(b)

Fig. 16 (a) Reflection phase graph of D-AMC surface for incident angle variation. Also shown are the final optimized dimensions of AMC unit. (b) Fabricated layer-by-layer FR4 PCB prototypes to realize the D-AMC metasurface design for verifying the concept (unit: millimeter).

The antenna and AMC reflector surfaces are fabricated by screen-printing silver ink on latex substrates. The Yagi antenna is printed on 1 mm-thick latex, while the S-AMC is fabricated using 3 mm-thick ground latex substrate. The D-AMC is fabricated using two 1.5 mm-thick latex substrates for each layer, thus the S-AMC and D-AMC surfaces have a total thickness of 3 mm. Commercially available flexible Styrofoam ($\varepsilon_r \approx 1$) of 5.5 mm thickness is used to separate the AMC surface from the Yagi radiator for both the YAGIS−AMC and YAGID−AMC antenna prototypes (as shown in Fig. 17).

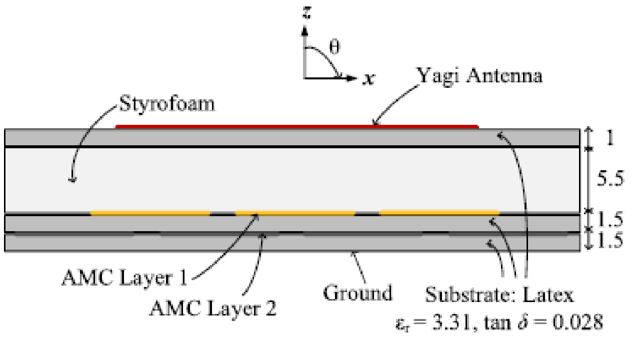

Fig. 17. Cross-sectional view of proposed Yagi-antenna over double layered AMC surface: YAGID-AMC.

The return loss for each Yagi antenna configuration is shown in Fig. 18 for both free-space and on-voxel chest location conditions. It can be observed that resonance deteriorates for antenna configurations without AMC when they are placed close to the voxel model. Note that the Yagi antenna is placed at a larger separation distance of 11.5 mm from the surface of the skin to maintain the same separation distance for all simulated radiators. A small shift to a lower frequency of 2.4 GHz is observed for the $\text{YAGI}_{\text{S-AMC}}$ when placed on voxel as compared to its resonance in free space at 2.45 GHz.

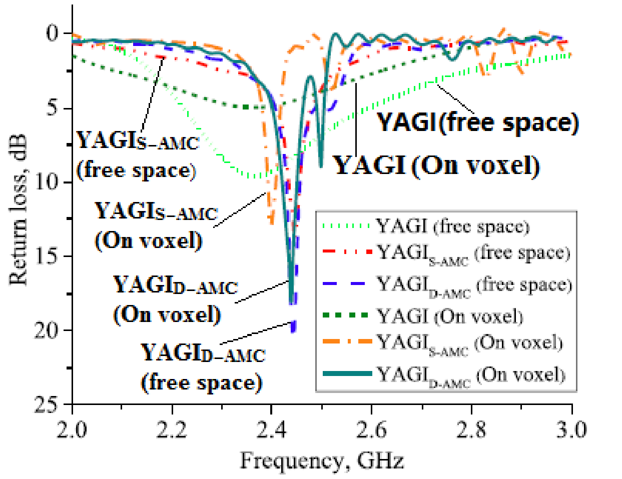

Fig. 18. Simulated return loss graph for the antenna configurations without and with AMC for free-space and on-voxel (chest) surrounding conditions.

The antenna efficiency drops from 86% (in free space) to 29.39% when the Yagi antenna is placed on the voxel chest without AMC structure. The antenna efficiency improves to 74.82% for the $\text{YAGI}_{\text{S-AMC}}$(free space) antenna configuration and $\text{YAGI}_{\text{D-AMC}}$ shows a further improvement in antenna efficiency to 78.97%. Various recorded values for peak SAR levels for all body locations for an input power of 1 W are summarized in Table I for all three antenna configurations.

Table I. SIMULATED PEAK SAR VALUES FOR DIFFERENT ANTENNA CONFIGURATIONS (INPUT POWER = 1 W)

Antenna configurations	Chest (W/kg) 1-g tissue	Chest (W/kg) 10-g tissue	Arm (W/kg) 1-g tissue	Arm (W/kg) 10-g tissue	Leg (W/kg) 1-g tissue	Leg (W/kg) 10-g tissue
YAGI	11.4	4.2	18.3	6.76	3.04	1.75
$\text{YAGI}_{\text{S-AMC}}$	2.06	1.24	1.95	1.31	0.271	0.134
$\text{YAGI}_{\text{D-AMC}}$	1.47	0.714	1.81	1.16	0.211	0.111

Textile Antenna Incorporated with High Impedance Surface

A novel dual band textile antenna with operating frequencies of 2.4 GHz and 5.8 GHz is designed from a single band wearable Planar Inverted F Antenna (PFIA). Fig. 19 demonstrates the geometrical details of the proposed antenna [18].

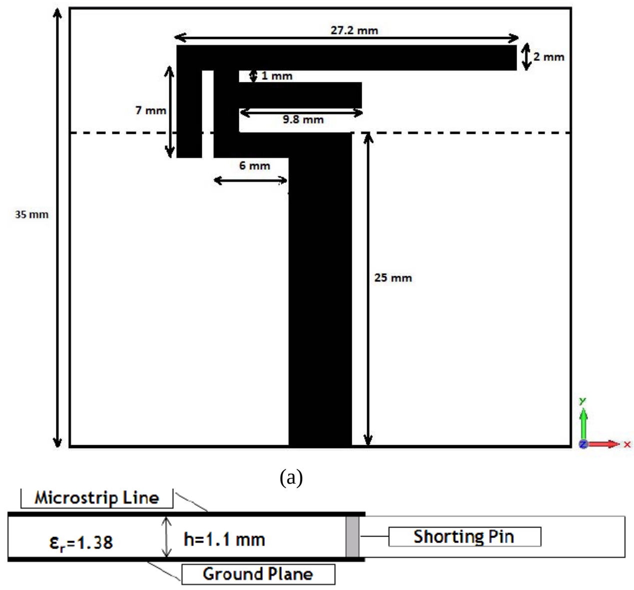

Fig. 19. Textile antenna configuration (a) Top view (b) Side view

This textile antenna has been integrated with a dual band high impedance surface (HIS), an array of 3×3 units (as shown in Fig. 20). Felt fabric is used for the substrate and conducting elements are modeled as felt.

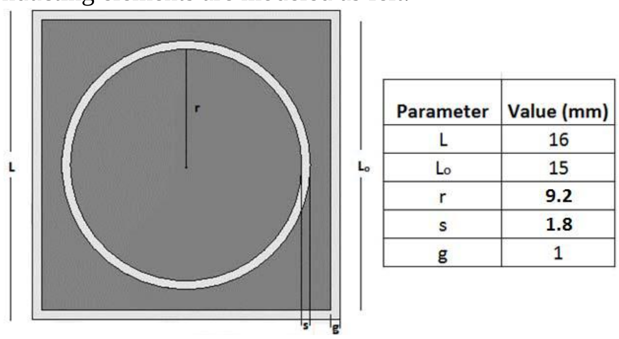

Fig. 20. Structure Geometry of dual band fabric HIS unit

The return loss of the combined design is presented in Fig. 21. It can be observed that return loss of the antenna/HIS combination has improved to -23 dB and -27 dB at 2.40 GHz and 5.80 GHz respectively, showing good impedance matching at these frequencies for the free space environment. When the integrated design is evaluated over body, there is negligible change in the operating frequencies as seen in Fig. 21. This is due to the incorporation of the HIS resulting in minimization of coupling between the antenna and the body.

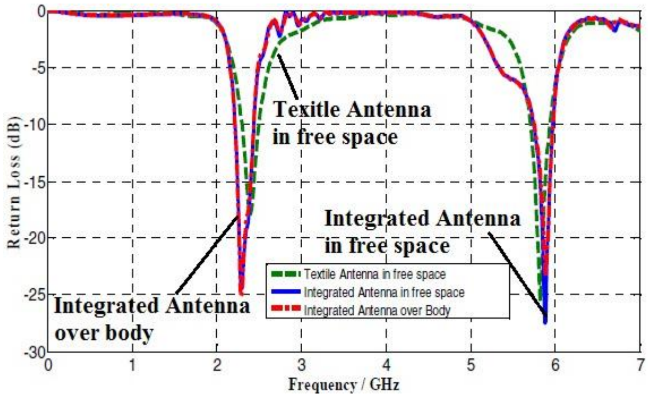

Fig. 20. Return loss comparison for antenna over body phantom with and without HIS

SAR has been calculated for 10 g tissue at both the operating frequencies for the antenna without HIS combination by placing it over body phantom. The values are 11.7 W/Kg and 2.39 W/Kg at 2.4 GHz and 5.8 GHz respectively. Following the combination of the textile antenna and HIS structure, new SAR values of 0.68 W/Kg and 0.069 W/Kg are obtained at 2.4 GHz and 5.8 GHz respectively which demonstrates the necessity of HIS for textile/wearable antennas.

Dual-band EBG Integrated Monopole Antenna

A monopole antenna operating at GSM-1800 MHz and ISM-2.45 GHz is proposed in [19], which is designed on jean fabric of thickness 1 mm. The antenna is backed with a 3×3 EBG array of dimension 150×150 mm^2. The dimension of dual band antenna and EBG unit are depicted in Fig. 21. The substrate material used for the EBG is also jean fabric. The unit cells and the ground plane are made of copper sheets.

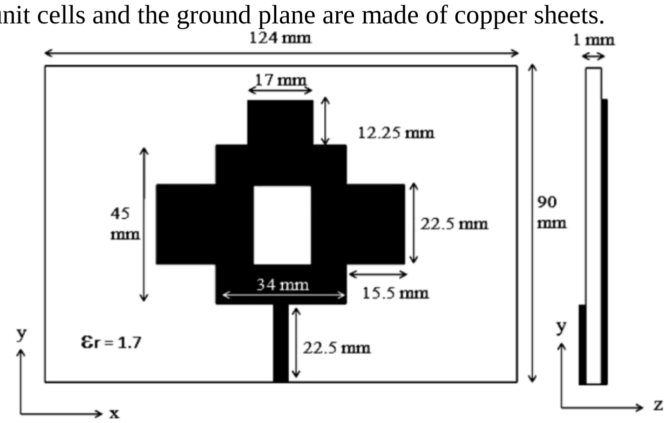

(a)

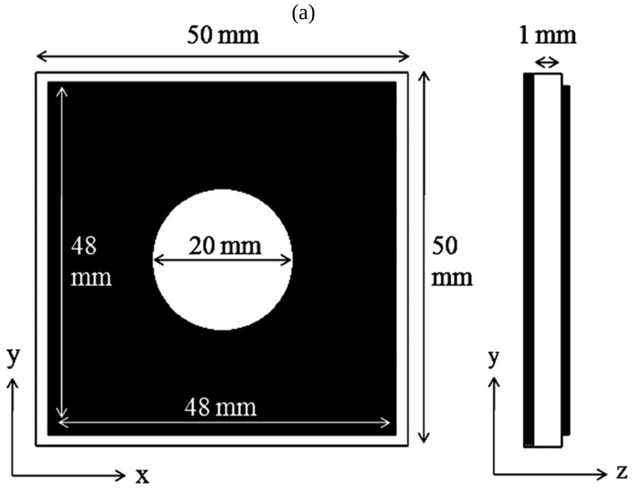

(b)

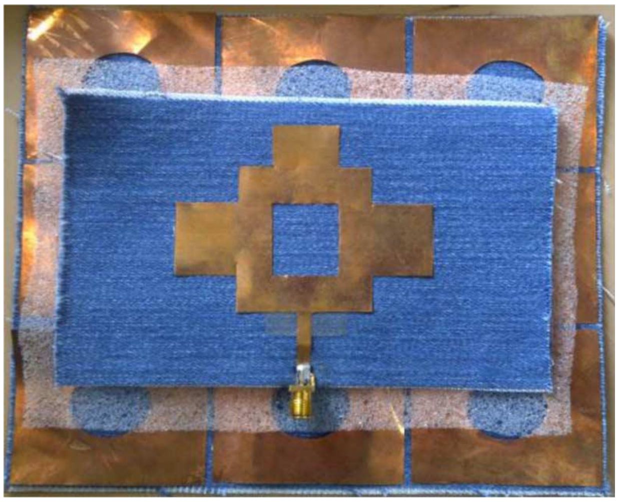

(c)

Fig. 21. (a) Dimension details of the monopole antenna (b) Dimension of the EBG unit cell (c) Fabricated prototype

The reflection coefficient plot of the antenna measured in free space with and without EBG is depicted in Fig. 22. For the antenna with EBG, the first band ranges from 1.78 to 1.98 GHz, with an impedance bandwidth of 200 MHz (10.92%). The second band is from 2.38 to 2.505 GHz with an impedance bandwidth of 125 MHz (5.08%).

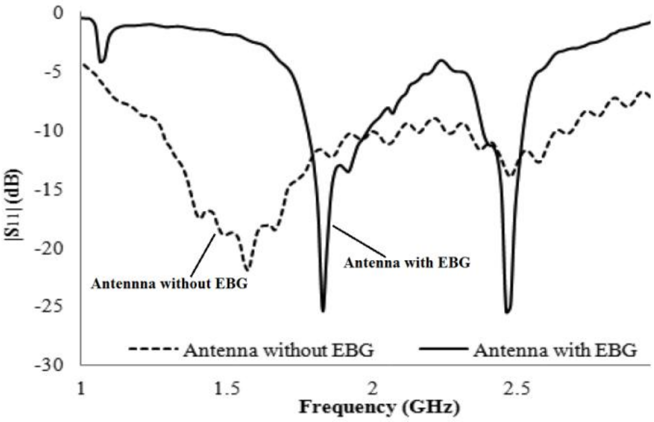

Fig. 22. Reflection coefficient characteristics of the antenna measured in free space.

Fig. 23 depicts the reflection coefficient characteristics of the antenna measured on-body with and without an EBG. The highly dielectric nature of the human tissue affects the response of the antenna without EBG, causing both attenuation and detuning. However, with the placement of the EBG, the desired bands of operation are obtained.

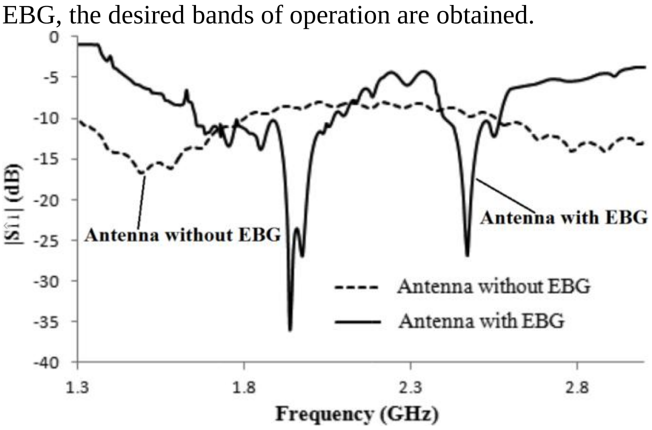

Fig. 23. Reflection coefficient characteristics of the antenna measured on body.

The SAR of the prototype is analyzed using a three-layered rectangular human body model. The SAR values at 1.8 GHz with and without EBG are 0.024 and 5.77 W/kg, respectively. At 2.45 GHz, the corresponding SAR values are 0.016 and 6.62 W/kg. A significant reduction in SAR in both the bands has been obtained using the EBG structure.

III. Some Challenges and Considerations

The patch antenna is a good candidate for wearable devices, since it is generally low profile and easy to fabricate. Using textile materials as substrates helps reduce surface wave losses and enhances the overall bandwidth. When a wearable textile antenna is worn on the human body, long term electromagnetic radiation poses potential health risks. Minimization of Specific Absorption Rate is therefore a challenge for wearable patch antennas.

Metamaterials including AMC, HIS and EBG structures, have their own advantages for wider bandwidths, reductions in backward wave energy and hence good SAR values [20-21]. The problems in the design of these structures, however, are the increasing overall antenna size and antenna fabrication complexity.

Additionally, antenna performance and robustness under deformations (bending, crumpling, wrinkling, wetting) have to be investigated and incorporated into the design of wearable antennas to meet conformal requirements.

IV. Conclusion

The antenna is an essential element in wireless body-centric networks for WBAN applications. Its complexity depends on the radio transceiver requirements and also on the propagation characteristics of the surrounding environment. Not only textile patch antennas but also antennas with metamaterial structures for wearable devices have their own merits and demerits. It is important to the continued improvement of WBAN applications to design optimized wearable antenna, balancing the trade-offs between an antennas performance and its size and complexity.

References

[1] M. Patel and J. Wang, "Applications, challenges, and prospective in emerging body area networking technologies," IEEE Trans. Wireless Commun., vol. 17, no. 1, Feb. 2010. pp. 80–88,

[2] Ramesh Garg, Prakash Bhartia, Inder Bahl, Apisak Ittipiboon, "Microstrip antenna design handbook", Artech House, 2001.

[3] L. Ma, R. M. Edwards and S. Bashir, "A Wearable Monopole Antenna for Ultra-Wideband with Notching Function", Wideband and Ultrawideband Systems and Technologies: Evaluating current Research and Development, 2008, pp. 1-5.

[4] B. Grupta, S. Sankaralingam, S. Dhar, "Development of Wearable and Implantable Antennas in the Last Decade: A Review". In Proceedings of Mediterranean Microwave Symposium (MMS), Guzelyurt, Turkey, 25–27 August 2010, pp. 251–267

[5] G. George, R. Nagarjun, D. Thiripurasundari, R. Poonkuzhali and Z. C. Alex, "Design of Meander Line Wearable Antenna", IEEE Conference on Information and Communication Technologies, 2013, pp. 1190-1193.

[6] The introduction of metamaterial is available at http://en.wikipedia.org/wiki/Metamaterial

[7] A. Erentok, and R. W. Ziolkowski, Chen "Metmaterial-Inspired efficient electrically small antennas," IEEE Trans. Antennas Propagat., vol. 56, no. 3, Mar. 2008, pp. 691-707.

[8] N. Hwang, and f. C. Chen "Reduction of the Peak SAR in the human head with Metamaterials," IEEE Trans. Antennas Propagat, vol. 54, no. 12, Dec. 2006, pp. 2113-2130.

[9] J. C. Wang, E. G. Lim, M. Leach, Z. Wang, K. L. Man and Y. Huang, "Conformal Wearable Antennas for WBAN Applications", *Proceedings of the International MultiConference of Engineers and Computer Scientists 2016*, IMECS 2016, 16-18 March, 2016, Hong Kong, pp.651-654.

[10] H. Nawaz, M. A. B. Abbasi, "On-body Textile Antenna Design and Development for Body-centric Wireless Communication Systems", International Bhurban Conference on Applied Sciences & Technology (IBCAST), 2015, pp. 650-653.

[11] M. E. Jalil, M. K. A. Rahim, N. A. Samsuri, N. A Murad, N. Othman, H. A. Majid, "On-body Investigation of Dual Band Diamond Textile Antenna for Wearable Applications at 2.45 GHz and 5.8 GHz", 7th European Conference on Antennas and Propagation, 2013, pp. 414-417.

[12] H Gidden, D.L Paul, G S Hilton and J. P McGeehan, " Influence of body Proximity on the Efficiency of Wearable Textile Patch Antenna," *the 6th European conference on Antennas and Propagation* (EUCAP), Prague 2012, pp. 1353-1357.

[13] E. F. Sundarsingh, S. Velan, M. Kanagasabai, A. K. Sarma, C. Raviteja, and M. G. N. Alsath, "Polygon-Shaped Slotted Dual-Band Antenna for Wearable Applications", IEEE Antennas and Wireless Propagation Letters, vol.13, 2014, pp. 611-614.

[14] M. A. R. Osman,M. K. A. Rahim,M. Azfar, N. A. Samsuri, F. Zubir, and K. Kamardin, "Design, implementation and performance of ultrawideband textile antenna," Prog. Electromagn. Res. B, 2011, vol. 27, pp. 307–327.

[15] W. A. M. Alashwal, K. N. Ramli, "Small Planar Monopole UWB Wearable Antenna with Low SAR", IEEE Region 10 Symposium, 2014, pp. 235-239.

[16] W. A. M. AlAshwal, K. N. Ramli, "Compact UWB Wearable Antenna with Improved Bandwidth and Low SAR", IEEE International RF and Microwave Conference, 2013, pp. 90-94.

[17] K. Agarwal, Y. X. Guo, B. Salam, "Wearable AMC backed near-endfire antenna for on-body communications on latex substrate", *IEEE trans on Components, Packaging and Manufacturing Technology*, vol. 6, no. 3, March. 2016, pp. 346-358.

[18] M. S. Khan, H. Ali, S. Bashir, L. M. Al-Hadhrami, K. U. Jan, "Textile antenna incorporated with high impedance surface for on-body performance enhancement", *the 8th European conference on Antennas and Propagation*, The Hague, 2014, pp 1413-1417.

[19] S. Velan, E. F. Sundarsingh, M. Kanagasabai, A. K. Sarma, C. Raviteja, R. Sivasamy, J. K. Pakkathillam, "Dual-band EBG integrated monopole antenna deploying fractal geometry for wearable applications", IEEE Antennas and Wireless Propagation Letters, vol. 14, 2015, pp. 249-252.

[20] J. H. Kim, H. M. Lee, "Low Specific Absorption Rate Wearable Antenna for WLAN Band Applications", Antenna and Propagation (EuCAP), 2010, pp. 1-5

[21] S. Yan, P. J. Soh, G. A. E. Vandenbosch, "Wearable Dual-Band Magneto-Electric Dipole Antenna for WBAN/WLAN Applications", Antennas and Propagation, IEEE Transaction, 2015, vol.63, no. 9, pp. 4165-4169.